Electrically Excitable Normal Rat Kidney Fibroblasts: A New Model System for Cell-Semiconductor Hybrids

W. J. Parak,* J. Domke,* M. George,* A. Kardinal,* M. Radmacher,* H. E. Gaub,* A. D. G. de Roos,# A. P. R. Theuvenet,# G. Wiegand,§ E. Sackmann,§ and J. C. Behrends¶

*Institut für Angewandte Physik, Ludwig-Maximilians Universität, Munich, Germany; #Department of Cell Biology, University of Nijmegen, Nijmegen, The Netherlands; §Physik Department E22, Technische Universität, Munich, Germany; and ¶Physiologisches Institut, Ludwig-Maximilians Universität, Munich, Germany

ABSTRACT In testing various designs of cell-semiconductor hybrids, the choice of a suitable type of electrically excitable cell is crucial. Here normal rat kidney (NRK) fibroblasts are presented as a cell line, easily maintained in culture, that may substitute for heart or nerve cells in many experiments. Like heart muscle cells, NRK fibroblasts form electrically coupled confluent cell layers, in which propagating action potentials are spontaneously generated. These, however, are not associated with mechanical disturbances. Here we compare heart muscle cells and NRK fibroblasts with respect to action potential waveform, morphology, and substrate adhesion profile, using the whole-cell variant of the patch-clamp technique, atomic force microscopy (AFM), and reflection interference contrast microscopy (RICM), respectively. Our results clearly demonstrate that NRK fibroblasts should provide a highly suitable test system for investigating the signal transfer between electrically excitable cells and extracellular detectors, available at a minimum cost and effort for the experimenters.

INTRODUCTION

Cell semiconductor hybrids are of great interest for a large variety of applications, such as monitoring electrical communication within neuronal networks or other electrically active cellular aggregates or the development of new neuronal prostheses. In principle, they provide for noninvasive, simultaneous, and spatially resolved recordings with long-term stability of bioelectrical activity from multiple single cells (Denyer et al., manuscript submitted for publication; Gross et al., 1997). These requirements are obviously not met by classical microelectrode or patch-clamp recording techniques. Optical recording using voltage-sensitive dyes, while enabling simultaneous recording from different locations, cannot be considered noninvasive, because it will eventually result in photodynamic damage of cells (Schaffer et al., 1994).

At present, two extracellular recording techniques are available that are based on cells adherent to semiconductor-detectors or planar metal electrodes. When electrically excitable cells are close to the gate electrode of a field effect transistor (FET), their action potentials can steer the source drain current (Bergveld et al., 1976; Fromherz et al., 1991). Another possibility is to adhere cells close to planar, extracellular microelectrodes, such as thin wires made of indium-tin-oxide (ITO) or platinized gold (Gross et al., 1985, 1995; Jimbo et al., 1993; Regehr et al., 1989) and measure their electrical activity either as ohmic or transient currents. With both techniques, signal transduction between single neurons of invertebrates (e.g., leeches (Fromherz et al., 1991; Wilson et al., 1994) or snails (Gross et al., 1977; Novak, 1986; Regehr et al., 1989)) and the extracellular detector is possible. The signal-to-noise ratio is typically better than 1000.

Gross et al. were able to monitor action potentials from mammalian neuronal tissue adhered to extracellular microelectrodes (Gross et al., 1995, 1997). Furthermore, the groups of Fromherz and Offenhäusser could record electrical activity from single mammalian neurons maintained 3–5 days in vitro (DIV) with FETs, which were stimulated with artificial test pulses by patch clamp (Offenhäusser et al., 1997; Vassanelli and Fromherz, 1997; Vassanelli and Fromherz, 1998). At present an important aim is still to improve recordings of defined action potentials from single mammalian neurons under natural conditions. New semiconductor designs with enhanced sensitivity will be needed to reach this goal.

In addition to neurons, action potentials from layers of heart muscle cells have been detected with FETs (Sprössler et al., manuscript submitted for publication) and extracellular microelectrodes (Connolly et al., 1990; Denyer et al., manuscript submitted for publication; Israel et al., 1984, 1990; Thomas et al., 1972), respectively. Heart muscle cells have been proved to be very stable systems for extracellular potential recordings and can be used for drug screening assays, correlating changes in beating intervals with the amount of added pharmaceutical agents (Denyer et al., manuscript submitted for publication). With cardiomyocytes, electrical activity is necessarily associated with mechanical movement. Depending on the principle of measurement used, electromechanical coupling may thus introduce artificial signals.

Unfortunately, all of the cell systems described above are primary cultures and thus have to be freshly prepared for each experiment. Clearly, an electrically excitable cell system that could be kept in culture and could be easily grown

Received for publication 27 April 1998 and in final form 28 October 1998.

Address reprint requests to Dr. Hermann E. Gaub, Institut für Angewandte Physik, Ludwig-Maximilians Universität, München, Germany. Tel.: 49-89-2180-3173; Fax: 49-89-2180-2050; E-mail: gaub@physik.uni-muenchen.de.

0006-3495/99/03/1659/09 $2.00

on extracellular recording devices would be a very convenient means of testing new generations of cell-semiconductor hybrids.

Recently it was found that normal rat kidney (NRK) fibroblasts can behave like an excitable tissue (deRoos et al., 1997a,b, 1998). These fibroblasts can easily be kept in culture and grow under standard cell culture conditions. In these monolayers, Ca^{2+} action potentials can be generated by depolarization with either bradykinin or an elevation of the extracellular K^+ concentration. When only a part of the monolayer is depolarized by a localized addition of high K^+, a propagating action potential is generated that travels at a speed of ~6 mm/s through the monolayer (deRoos et al., 1998). These action potentials are characterized by an upstroke to positive membrane potentials and are carried by Ca^{2+}, but can also be carried by Sr^{2+} ions through Ca^{2+} channels. After a plateau phase (or shoulder) due to the opening of Ca^{2+} activated Cl^- channels, cells finally return by repolarization to resting levels. Besides stimulated action potentials, NRK fibroblasts can exhibit spontaneous Ca^{2+} action potentials, leading to synchronized Ca^{2+} spiking (deRoos et al., 1997a). Unlike heart muscle cells and neuronal cells, these action potentials appear to have no Na^+ component, and the duration of the action potential is much longer in NRK fibroblasts.

Two sets of properties are central to the potential usefulness of a cell type in testing cell-semiconductor hybrids: 1) its electrical excitability and 2) its adhesion to the detector surface. Here we used the whole-cell configuration of the patch-clamp technique to assess the amplitude and time course of action potentials. Atomic force microscopy (AFM) (Henderson et al., 1992; Radmacher et al., 1992) is an established technique that enables the micromorphological study of living cells. We make use of this technique in this study to determine the shape, height profile, and adherence of cells growing on semiconductor wafers. The immediate zone of adhesion, in turn, can be imaged by reflection interference contrast microscopy (RICM) (Izzard and Lochner, 1976; Schindl et al., 1995; Simson et al., 1998), where, in close analogy to the formation of Newton's rings (Hecht, 1987), optical interference is measured between cell and substrate.

MATERIALS AND METHODS

Cell culture

As substrates silicon chips (Cytosensor Microphysiometer chips; Molecular Devices Corporation, Sunnyvale, CA) covered with SiO_2/Si_3N_4 and glass microscope cover slides (Assistent, Munich, Germany) were used. They were cleaned by sonification successively in ethanol, Millipore water (Milli-Q plus 185; Millipore, Eschborn, Germany), detergent (2% Hellmanex II, no. 320.001; Hellma GmbH, Müllheim, Germany), and KOH dissolved in ethanol solution and two times in Millipore water. All substrates used for heart cell cultures were coated with fibronectin to improve cellular adhesion. Because the aim of this paper is to compare the properties of NRK fibroblasts with heart muscle cells as a reference system, we adopted the fibronectin coating protocol from reports, in which recordings of extracellular potentials were reported (Denyer et al., manuscript submitted for publication; Sprössler et al., manuscript submitted for publication).

NRK fibroblasts (clone 49F) were seeded at a density of 10^{+4} cells/cm^2 on uncoated glass or silicon substrates, respectively, and grown to confluence in bicarbonate-buffered Dulbecco's modified Eagle's medium (DMEM, Gibco no. 31966) supplemented with 10% newborn calf serum (no. N-4637; Sigma, Deisenhofen, Germany) and 1% penicillin-streptomycin (Sigma no. P-7539). Confluent cultures were made quiescent by incubating them in serum-free DF medium (DMEM/Ham's F12, 1:1, Gibco no. 11321; Life Technologies GmbH, Eggenstein, Germany) supplemented with 30 nM Na_2SeO_3 (Gibco no. 13012), 10 μg/ml human transferrin (Gibco no. 13008), and 1% penicillin-streptomycin.

Heart muscle cells were prepared according to the protocols of Riehle et al. and Denyer et al. (Denyer et al., manuscript submitted for publication; Riehle and Bereiter-Hahn, 1994). Briefly, hearts were extracted from 7–9-day-old chicken embryos and enzymatically dissolved. The cell suspension was then transferred in a tissue culture flask and incubated for 1 h. This incubation allowed the majority of fibroblasts to adhere to the flask, leaving an increased proportion of ~80% myocytes in suspension (Blondel et al., 1971). Finally, heart cells were plated on substrates at densities of $25–30 \times 10^{+4}$ cells/cm^2 and incubated for 24 h. Every 2 days, medium was exchanged with new M199 medium (Gibco no. 21183), supplemented with 2% of 1 M HEPES, 0.5% of 7.5%-$NaHCO_3$, 0.5% ITS (Gibco no. 41400), 1.5% of 200 mM L-glutamine, 1% penicillin-streptomycin solution, 0.13% amphotericin B solution, and 3% fetal calf serum (pH 7.5). After 1–2 days in vitro (DIV), large areas of the confluent cell layers started beating. All measurements were made after 1–4 DIV.

Patch clamp

Current clamp was applied with an EPC7 patch-clamp amplifier (List, Darmstadt, Germany), using the whole-cell configuration (Hamill et al., 1981) (see Fig. 1). All measurements were made on confluent cells grown on silicon wafers at room temperature without CO_2 control.

NRK fibroblasts

Cells were incubated in a nominally Ca^{2+}-free DF medium supplemented with 3 mM Sr^{2+} as previously described (deRoos et al., 1998). Using Sr^{2+} as a charge carrier ensured a very consistent action potential generation (>90% of the experiments). Action potentials were evoked by adding a small volume (5–10 μl) of 120 mM K^+ at a distance (usually 10–20 mm) from the patch-clamp pipette as previously described in detail (deRoos et al., 1998). Pipettes were filled with a high-K^+, Tris-buffered solution (in mM: 25 NaCl, 120 KCl, 1 $CaCl_2$, 1 $MgCl_2$, 10 Tris, 3.5 EGTA, pH 7.4).

Heart muscle cells

Spontaneous action potentials were recorded at parts of the cell layer where no contraction was visible. Pipettes were filled with a high-K^+ solution (Risso and DeFelice, 1993) (in mM: 120 KCl, 0.1 $CaCl_2$, 2 $MgCl_2$, 1.1 EGTA, 10 HEPES, 30 D-glucose).

Atomic force microscopy

AFM was performed with a commercial instrument (Bioscope; Digital Instruments, Santa Barbara, CA) (see Fig. 1). All experiments were made on cells grown on silicon wafers. Wafers were glued in 35-mm culture dishes, which were then filled with culture medium. Silicon nitride cantilevers (Microlevers; Park Scientific, Santa Clara, CA) were used as AFM tips. These had a force constant of 8 mN/m, calibrated by the thermal noise method (Butt and Jaschke, 1995). For obtaining elastic properties and the real topography of the investigated sample, the force mapping mode (Cleveland et al., 1995) was employed: force curves were taken while the tip was raster-scanned laterally over the sample. As described in great detail previously (Domke and Radmacher, 1998), fitting the force curves with the Hertz model yields a quantitative value of the elastic (Young's)

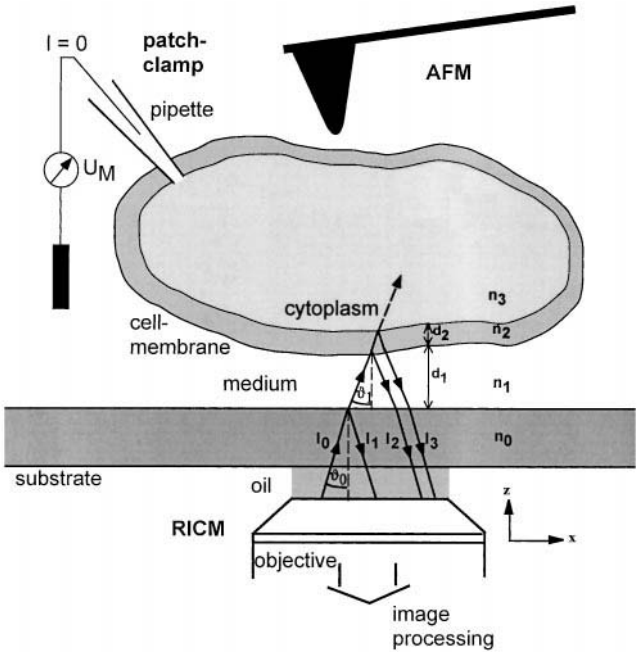

FIGURE 1 Sketch of applied techniques. Experiments were actually done with three different setups. Electrical properties were investigated with patch clamp in current clamp mode. With the pipette current I held at zero, membrane potential U_M is measured with a feedback loop. AFM measurements were performed by scanning the tip of a cantilever across the cell. Image formation in RICM is realized as follows. Monochromatic light reflected from the substratum (I_1) interferes with light reflected from the different interfaces of the cell (I_2, I_3, . . .) and cell organelles, respectively. The resulting local intensity $I(x,y)$ of the light reflected from the observed object depends on the total reflectivity of the object. Because of the finite aperture of illumination, light from different angles of incidence ϑ has to be considered. In different media the maximum illumination angle $\theta_i = \max(\vartheta_i)$ can be calculated from the illuminating numerical aperture (INA), and the refractive index of the medium n_i by INA $= n_i \sin(\theta_i)$.

modulus and the real height of the sample. Because this evaluation needs force curves recorded on cells and on the uncovered substrate, subconfluent cells were used.

Reflection interference contrast microscopy

The principle of image formation (Gingell and Todd, 1979; Rädler and Sackmann, 1993; Wiegand et al., manuscript submitted for publication) is illustrated in Fig. 1. To discriminate between light reflected from the contact zone between cell and substrate and from the organelles and the backside of the cells, one can change the illuminating numerical aperture (INA) (Verschueren, 1985). At high INA values, reflections in the close proximity of the substrate surface dominate the measured intensity $I(x, y)$ (Gingell and Todd, 1979; Wiegand et al., manuscript submitted for publication). Multireflections were neglected because of the low reflectivity of the particular interfaces. If one would assume in first order that only light I_2 from the medium/cell-membrane interface interferes with the reference intensity I_1 (neglecting I_3, I_4, . . .) and that the interface is parallel to the substrate surface, then $I(x, y)$ would be a cosine transformation of the local distance $d_1(x, y)$ between cell and substrate. As a consequence of the higher refractive index of the cell membrane (n_2) than the index of the surrounding medium (n_1), light reflected from the buffer/cell interface experiences a phase shift of $\delta = \pi$. Therefore, the areas of close contact of an adhering cell appear dark in RICM.

All experiments were made with subconfluent cells grown on glass cover slides. The microscope setup used for the present experiments was a modified (Pluta, 1988) Zeiss Axiomat microscope (Oberkochen, Germany). Monochromatic epi illumination was provided by a 100-W high-pressure mercury lamp and a bandpass filter ($d\lambda = 5$ nm, 85% peak transmission) selecting the green 546.1-nm line. Field and aperture stops were adjusted to an INA of 0.75. The microscope was equipped with a Zeiss Neofluar 63/1.25 Antiflex objective and two polarizers. The antiflex technique (Schindl et al., 1995) was used to eliminate stray light in the microscope, which could obscure the low intensity (1%) of the reflected light. RICM images were recorded with a CCD camera (HR480, Aqua TV; Germany), preprocessed with a Datacube image-processing system (Datacube Peabody, Boston, MA), and stored with a S-VHS video recorder (AG7350; Panasonic). A video board (Perceptics, Knoxville, TN) was used to digitize the images into 256 gray levels, and image processing was carried out with the software NIH Image (Wayne Rasband, National Institutes of Health, Bethesda, MD). For static image analysis the data were averaged over four to eight frames to reduce camera noise.

RESULTS

Typical action potentials recorded with patch pipettes in the current clamp mode are shown in Fig. 2. NRK cells showed an action potential rising from a resting membrane potential

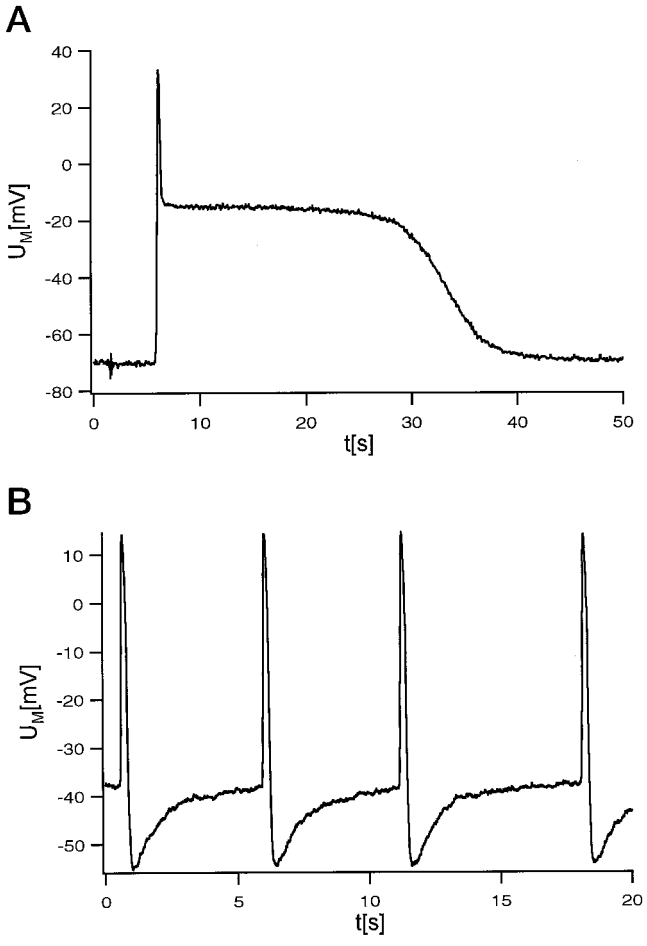

FIGURE 2 Membrane potential U_M versus time t, recorded with current clamp on confluent cell layers adhered to silicon substrates. Data were filtered with 1 kHz. (*A*) NRK fibroblasts. (*B*) Chicken heart cells.

of −64 ± 7 mV (n = 11; all values are given including their standard deviation) to a peak of 35 ± 5 mV. This yields a maximum change in membrane potential of 99 ± 9 mV. The rapid phase of the action potential was followed by a plateau phase lasting 39 ± 11 s. During the upstroke of the action potential, the rate of depolarization was 1.2 ± 0.3 V/s. These results show that action potentials can be generated when the cells were grown on wafers, and they had characteristics similar to those already described.

Cardiac pacemaker cells had a maximum diastolic potential of −59 ± 7 mV (n = 7). Spontaneous action potentials occurred at intervals of between 500 ms and several seconds and reached +8 ± 6 mV, corresponding to an amplitude of 67 ± 9 mV. The maximum rate of rise was 1.6 ± 0.7 V/s.

Because nontransparent silicon wafers were used, AFM had to be performed without the help of an optical microscope, and thus cells could not be visually selected. Furthermore, in cultures of cardiomyocytes, a comparatively large number of dead or loosely adherent cells were present. Consequently, the AFM tips had to be changed often because of contamination.

Typical AFM images of living NRK fibroblasts and heart cells are shown in Fig. 3. They were recorded in constant deflection mode with a loading force of ~1–2 nN. Simultaneously recorded height (Fig. 3, *A*, *C*) and deflection data (Fig. 3, *B*, *D*) are presented. The height signal is derived from the piezo's feedback loop that is used to keep the loading force of the AFM tip constant and corresponds to

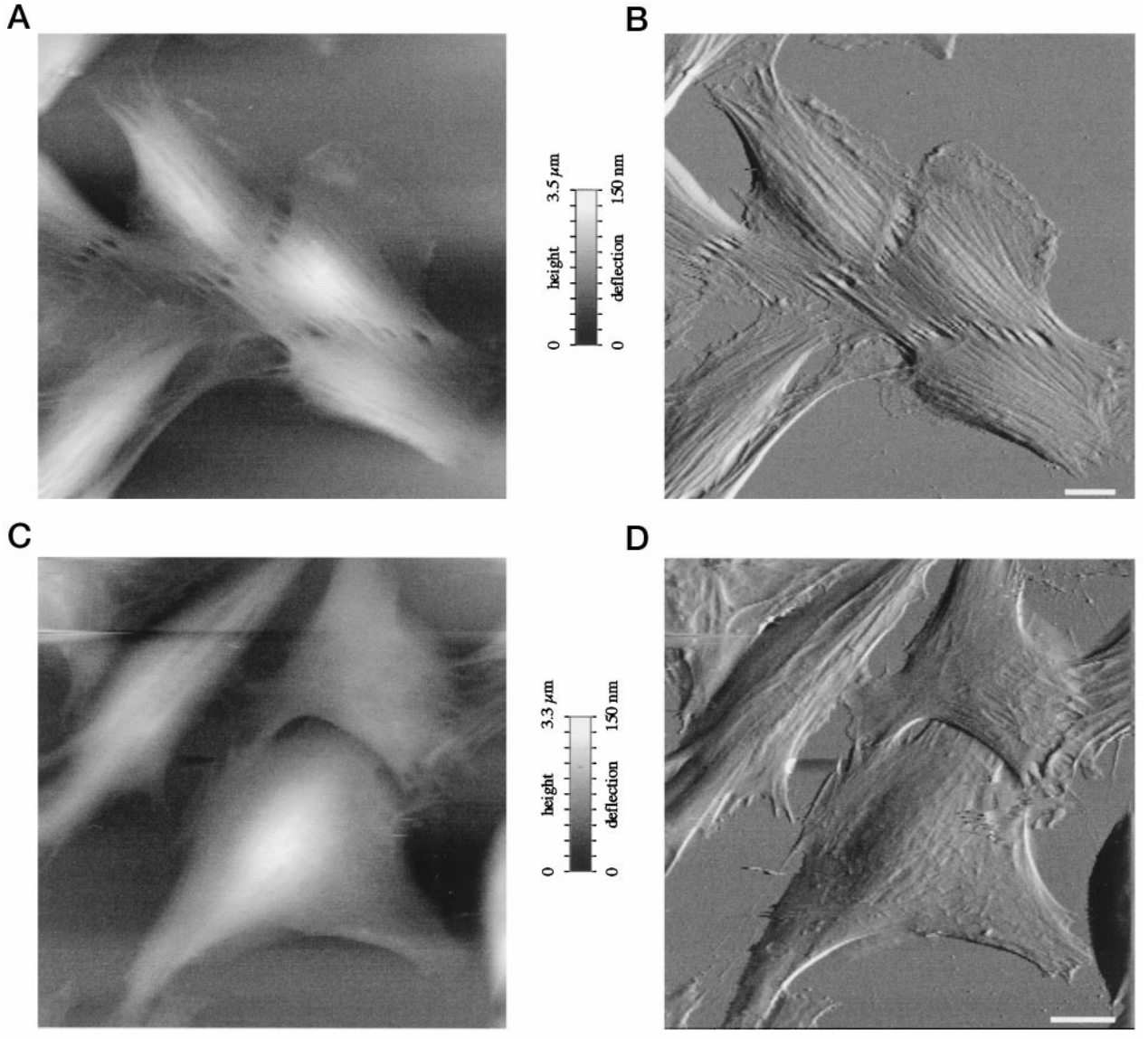

FIGURE 3 AFM images of a group of living NRK fibroblasts (*A*, *B*) and cardiomyocytes (*C*, *D*) adhering to silicon substrates recorded in contact mode. The baseline corrected height images (*A*, *C*) show the rough topography of the cells. The deflection images (*B*, *D*) present small surface corrugations of the sample. Because of a loading force of ~1–2 nN, cytoskeletal structures located under the cell membrane (e.g., stress fibers) are clearly visible, especially in the case of NRK fibroblasts. The scale bar represents 10 μm.

the rough topography of the sample. Because the feedback loop has a finite time constant, small deviations in the surface topography show up as deflections of the cantilever and form the deflection signal.

Cell length (l) and breadth (b), as well as substrate area covered (A) are given directly by the images. Values obtained for heart cells ($n = 11$) were $l = 72 \pm 22$ μm, $b = 34 \pm 13$ μm, $A = 1300 \pm 500$ μm^2. For fibroblasts ($n = 7$) we found $l = 64 \pm 19$ μm, $b = 37 \pm 15$ μm, $A = 1700 \pm 400$ μm^2. In contrast, the height values were reduced by a factor of ~25% because of compression by the cantilever tip. By fitting the force curves with the Hertz model (see Materials and Methods), the real height (h) of cells was obtained: $h = 2.9 \pm 0.7$ μm for heart cells and $h = 3.6 \pm 0.6$ μm for fibroblasts.

To further characterize the morphology of these cells, we introduced two shape parameters: one to measure the tendency of cells to be oblong ($s_1 = l/b$), so that for a disk-shaped ellipsoid ($l = b$) $s_1 = 1$, and for a cigar-shaped ellipsoid ($l \gg b$) $s_1 \to \infty$. Another parameter was used to describe flatness ($s_2 = (\pi/8)^{1/2} h/A^{1/2}$), where for a sphere-like ellipsoid ($l = b = h$, $A \propto l \times b$) $s_2 = 1$, and for a disk-like ellipsoid ($h \ll l, b$) $s_2 = 0$. The results obtained from AFM measurements were $s_1 = 2.1 \pm 1.1$, $s_2 = 0.050 \pm 0.015$ for heart cells and $s_1 = 1.7 \pm 1.3$, $s_2 = 0.055 \pm 0.011$ for fibroblasts.

RICM measurements were carried out on ~100 cells from seven different preparations (selected pictures are shown in Fig. 4). Single NRK fibroblasts could be easily identified, and dark areas, which correspond to the regions of closest contact (focal contacts; Izzard and Lochner, 1976) could be localized in nearly every cell. In RICM images with NRK fibroblasts, focal contacts were found to be distributed throughout the whole underside of cells, comprising $16 \pm 5\%$ ($n = 10$) of the total area of the membrane facing the substrate.

To obtain a quantitative estimate of cell-substrate separation, we used a model containing the following four refractive layers (Schindl et al., 1995), with their respective refractive indices chosen to best approximate the experimental data: glass substrate ($n_0 = 1.53$), liquid medium ($n_1 = 1.33$), cell membrane ($n_2 = 1.45$), and cytoplasm ($n_3 = 1.35$). The optical thickness of the membrane (d_2) was assumed to be 10 nm. Such a model allows the calculation of reflected light intensity (I) as a function of cell-substrate distance (d_1) (Rädler and Sackmann, 1992, 1993). Because the function relating these parameters is periodic with the wavelength of the light source, a given intensity cannot be unequivocally identified with a distance. For the purpose of this work, we assumed that d_1 in the focal contacts was below the first intensity maximum. This assumption seems reasonable, as otherwise distances of >200 nm would have been required to explain the measured low intensities of reflected light. Our standard model gave a mean cell-surface distance inside the focal contacts of 30 nm. This value showed variations between different focal contacts of the same cell of ± 15 nm ($n = 10$ focal contacts). Between means of different cells variation was ± 20 nm ($n = 10$ cells). To estimate errors associated with this approach, the optical parameters were systematically varied: changes of ~1% in one of the parameters, of which the most influential was n_3, yielded changes of up to $\pm$ 25 nm in d_1.

The shape of heart cells was less regular than that of NRK fibroblasts, and borders between different cells were often blurred. Generally, RICM pictures recorded with heart cells showed less contrast, and fewer focal contacts could be clearly identified. The relative membrane area taken up by focal contacts in cardiomyocytes was $6 \pm 3\%$ ($n = 10$). This value is significantly smaller than that obtained for fibroblasts. To improve adhesion, heart cells were grown on fibronectin-coated substrates (Denyer et al., manuscript submitted for publication; Sprössler et al., manuscript submitted for publication). A quantitative evaluation of the RICM data obtained for heart muscle cells therefore would have required the introduction of two additional parameters (n, d) in the optical model. However, in view of the error bars, no absolute values for the cell substrate distance are declared for cardiomyocytes.

Some RICM images recorded with cardiomyocytes showed large interference fringes, which are thought to represent light reflected at the upper cell membrane (Verschueren, 1985). They could be clearly differentiated from reflections at the lower membrane and did not affect the identification of focal contacts. In particular, during rhythmic contractions, those membrane areas that were identified as focal contacts did not change their interference pattern, whereas interference fringes widened, consistent with their origin at the upper membrane.

DISCUSSION

Action potentials in NRK fibroblasts have been described only recently (deRoos et al., 1998). It has also been demonstrated that opening of voltage-dependent L-type Ca^{2+} channels underlies the early fast phase of the action potential, whereas the plateau phase that lasts tens of seconds is likely to be mediated by Cl^- flux through Ca^{2+}-dependent Cl^- channels.

In the present study, cardiomyocytes derived from embryonic chick hearts showed action potentials with rise rates only slightly higher than that of fibroblasts. It is therefore likely that the cardiomyocytes studied here were pacemaker cells lacking fast voltage-dependent Na channels. For these, maximum slopes of action potentials well below 10 V/s have been described earlier at physiological temperatures (Jacobson and Piper, 1986; Kodama and Boyett, 1985; Nathan, 1986). The mean value of 1.6 V/s we obtained at room temperature, therefore, seems to be in good agreement with previous data. The kinetic similarity of the rising phases of fibroblast and cardiomyocyte action potentials is furthermore plausible, because in both cell types it is mediated by L-type Ca^{2+} channels.

Because the maximum height range of the piezo used for the AFM measurements was less than 6 μm, a preselection

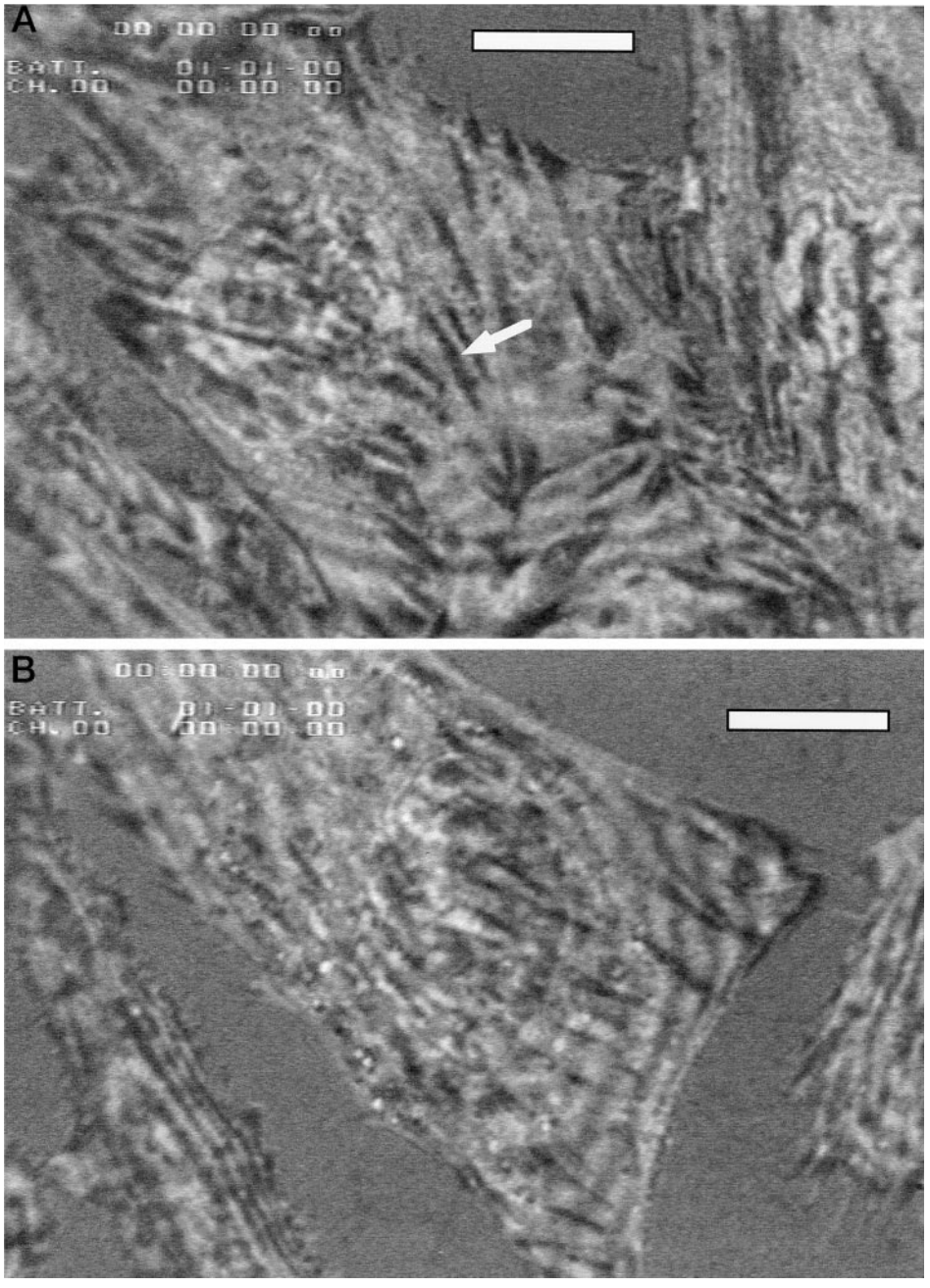

FIGURE 4 RICM picture, showing the adhesion zone between cells and glass substrate. Dark points correspond to areas with close contact. The scale bars represent 10 μm. (*A*) NRK fibroblasts. The arrow indicates a typical example for an area considered as focal contact. (*B*) Chicken heart cells.

of cells concerning their heights was made. In addition to the applied loading force, the AFM tip also exerts lateral shear stress on the cells. For both reasons, it is therefore likely that we preferentially selected cells that were well adhered to the substrate.

Because of the applied loading force the surface of the cells was compressed. Thus cytoskeletal structures from beneath the cell membrane became visible. Especially in the case of the NRK fibroblasts, stress fibers, i.e., bundles of actin filaments, could be clearly resolved (see Fig. 3 *B*), illustrating the need to use force maps to correctly estimate the true sample height. Analyzing force maps makes it possible to calculate the point where the AFM tip first touches the sample and thus to reconstruct the real topography of the cells. Comparison of heights obtained from force curve analysis with the raw height images consequently showed marked discrepancies. For instance, the height calculated from the force map of the fibroblasts of Fig. 3 was ~4.2 μm, but the same cell appeared to be 2.6 μm high in contact mode.

Summarizing the results of the morphological analysis using the AFM, it is clear that fibroblasts have a larger surface area and are less oblong and less flattened than cardiomyocytes.

Measuring the cell-substrate distance with RICM yielded clear differences between NRK fibroblasts and heart muscle cells in that focal contacts were more abundant and widespread in NRK fibroblasts than in cardiomyocytes.

Focal contacts have been described in a variety of cells as their closest contacts to substrate (Alberts et al., 1994, p. 841), where distances are reduced to a few tens of nanometers. Our result (30 ± 25 nm) is in reasonable agreement with the values most often cited in the literature (10–15 nm; (Izzard and Lochner, 1976).

It should be noted in this respect that absolute values are highly influenced by the optical model selected for the analysis of RICM data. For instance, highly divergent refractive indices, especially for the cytoplasm, can be found in the literature (Izzard and Lochner, 1980; Schindl et al., 1995; Verschueren, 1985). Furthermore, it has been argued that the refractive index of cellular compartments may be inhomogeneous. For instance, it may be higher than average at focal contacts, because of an enrichment in actin filaments (Bereiter-Hahn et al., 1979).

In addition, the multiple layers used in the model are defined as optical entities, not as pure cell biological compartments. Thus the value of 10 nm assumed for the membrane thickness would comprise both the intracellular actin network and the extracellular glycocalyx and is therefore larger than estimates of the thickness of a pure lipid bilayer (Johnson et al., 1991; Rädler and Sackmann, 1993), which yield ~3–5 nm.

An additional result of the RICM observations is that interference fringes attributed to reflection at the upper membrane were more frequently observed with cardiomyocytes but hardly ever with NRK fibroblasts. Reflections from the upper face of the membrane are to be expected only from very flat cells (Verschueren, 1985). This finding thus correlates well with our AFM data, which also indicate that heart cells were much flatter.

In conclusion, RICM has shown that NRK fibroblasts form a denser array of focal contacts with the substrate than heart muscle cells, and that the latter appear to be significantly less extended into the third dimension.

An advantage of the RICM technique lies in the fact that it provides a direct image of the cell's adhesion profile. Alternative techniques for quantitative determination of cell-substrate distances include total internal reflection fluorescence (TIRF) (Axelrod, 1981; Axelrod et al., 1984; Gingell et al., 1985; Hornung and Fuhr, 1996; Hornung et al., 1996) and fluorescence interference-contrast microscopy (FLIC) (Braun and Fromherz, 1997; Lambacher and Fromherz, 1996). Like RICM, TIRF can only be used with glass supports; FLIC, however, is usable with illumination from above and can therefore be applied to objects on opaque material like silicon. To date, FLIC has only been used with cells of a simple geometry.

The adhesion to substrate is one of the key components of success of any model for a cell-semiconductor hybrid. In this respect, the relevance of the RICM data obtained with glass substrates to the question of cell adhesion to silicon substrates merits discussion. As will be shown below, available data suggest that the two materials are equivalent regarding 1) chemical composition, 2) roughness, and 3) surface charge density.

Highly inert borosilicate coverslips were used as the glass substrate (Schott D263M glass: 64.1% SiO_2, 8.4% B_2O_3, 4.2% Al_2O_3, 6.4% Na_2O, 6.9% K_2O, 5.9% ZnO, 4.0% TiO_2, 0.1% Sb_2O_3). In contact with electrolytic solution, the surface of SiO_2 is formed by silanol sites. The manufacturing process for the silicon chips with a SiO_2/Si_3N_4 surface, as used here, has been described by Bousse et al. (1990). Because the authors claim that Si_3N_4 surfaces in contact with electrolytic solution comprise less than 2% amine sites and more than 98% silanol sites (Bousse and Mostarshed, 1991), SiO_2 and Si_3N_4 surfaces seem to have very similar reactive sites. To our knowledge, no specific chemical reactions of cellular components with the surface sites of borosilicate glass or silicon wafers with nitride surface have been reported. Therefore it seems reasonable to assume that glass substrates used with RICM experiments had surface sites similar to those of the silicon substrates used with the AFM and patch-clamp experiments.

The roughness of glass slides and silicon wafers was determined on the nanometer scale with the AFM by recording height profiles $H(x, y)$ across the substrate surface. Because substrates could have a slightly inclined orientation toward the x-y plane, only height deviations $\Delta H(x, y)$ referred to the principal plane of the substrate were used for further calculations. We defined the roughness $\langle H \rangle$ of the substrate as the normalized integral over the absolute height deviation ΔH, as already implemented in the commercial AFM software:

$$\langle H \rangle = \frac{1}{\Delta x\, \Delta y} \int_{y=0}^{\Delta y} \int_{x=0}^{\Delta x} |\Delta H(x, y)|\, \mathrm{d}x\, \mathrm{d}y$$

With scan sizes of $\Delta x = \Delta y = 10\ \mu$m we obtained a mean roughness of $\langle H \rangle = 0.37 \pm 0.07$ nm ($n = 9$) for the silicon chips and of 0.39 ± 0.05 nm ($n = 8$) for the glass slides, which were used as substrates for the cells. The two roughnesses are equal within their error bars.

Charge densities of a surface in electrolytic solution are often expressed in terms of the pH at the point of zero charge (pH_{pzc}). For $pH > pH_{pzc}$ and $pH < pH_{pzc}$, the surfaces are negatively and positively charged, respectively. In contact with electrolyte, the surface of silicon nitride is composed of both silanol sites (Si-OH) and primary amine sites (Si-NH_2) (Harame et al., 1987), whereas the surface of silicon oxide consists only of silanol sites. Because the pH_{pzc} found for silicon nitride surfaces (2–4) is not very different from silicon oxide surfaces, Bousse et al. conclude that "the surface of silicon nitride is practically the same as that of silicon oxide, and that virtually no ionizable amine groups remain at the surface" (Bousse and Mostarshed, 1991). Furthermore, Bousse et al. claim that "for properties such as biocompatibility or protein adsorption, . . . Si_3N_4 is expected to be very similar to SiO_2" (Bousse and Mostarshed, 1991). Therefore we conclude that there should be no significant difference in the surface charge density between silicon chips and glass slides.

As mentioned above, the cell-substrate distance of cells adherent to silicon wafers can be directly measured by the FLIC technique, which was recently introduced by Fromherz and co-workers (Braun and Fromherz, 1997). To our knowledge, to date only FLIC data obtained with erythrocytes have been published. It is useful to compare the distance between erythrocytes adherent to silicon substrates measured with the FLIC technique (Braun and Fromherz, 1997) with the distance between erythrocytes adherent to glass substrates, measured with the RICM technique (Donath and Gingell, 1983; Gingell and Todd, 1980; Gingell and Vince, 1979; Wolf and Gingell, 1983). Braun et al. obtained $d_1 = 12.4 \pm 0.7$ nm with erythrocytes adherent to polylysine-coated silicon chips with SiO_2 surface (Braun and Fromherz, 1997). Using the RICM technique, Gingel et al. estimated d_1 to be $\sim$10 nm with erythrocytes adherent to polylysine-coated RBC-glass at physiological salt concentrations (Gingell and Vince, 1979; Wolf and Gingell, 1983). As determined by the two techniques, these results indicate that at least for erythrocytes, the cleft between cells and substrate is on the same order of magnitude.

We have also shown in an additional patch-clamp control experiment that action potentials of heart muscle cells and NRK fibroblasts adherent to glass coverslips had the same characteristics as action potentials recorded with cells adherent to silicon wafers. Likewise, no differences were found—within error bars—between additional AFM data obtained with heart muscle cells and NRK fibroblasts adherent to glass substrates and the AFM data obtained with cells adherent to silicon wafers (data not shown).

Therefore, our RICM data, although obtained with cells on glass coverslips, are most likely relevant to the problem of cell adhesion on silicon wafers.

Cell-substrate adhesion is of crucial importance for signal transduction between cell and detector. We have therefore attempted in this study to quantitatively describe this parameter by two different approaches. It appears plausible that cellular adhesion depends on the distribution and density of focal contacts. One would equally expect flatness and oblong shape to be indicators of adhesion quality, as strong attraction between cell and substrate is required to overcome the cell's inherent tendency to adopt a rounded shape.

The conclusions to be drawn from this study regarding the quality of adhesion of NRK fibroblasts versus cardiomyocytes appear to depend on the point of reference: seen from below (RICM), NRK fibroblasts have a larger number and density of focal contacts. On the other hand, probing cells from above (AFM) yields data compatible with stronger substrate attraction acting on cardiomyocytes than on fibroblasts.

However, there is evidence that substrate adhesion is less stable in time for cardiomyocytes. We observed in several cases that, after 4 days in culture, an entire cell layer detached from the substrate and formed a ball-like agglomerate. A tendency to gradually lose adhesion so as to form a more rounded shape has been described earlier in cultured cardiomyocytes (Jacobson and Piper, 1986).

Our electrophysiological data indicate a close similarity between the action potentials of cardiac pacemaker cells and NRK fibroblasts. Because of their slow rise rate, only weak capacitative coupling to a detector is to be expected. The long duration of current flow and the large contact area, however, facilitate resistive coupling.

In conclusion, NRK fibroblasts offer many of the excitability properties of cardiomyocytes and show an adhesion profile that appears at least as strong and is likely to be more stable than that of heart muscle cells. In addition, the absence of contractions eliminates a possible source of artificial signals. As cell lines, NRK cells are easily obtained and cultured and provide standardized conditions that are difficult to realize with primary cell cultures. Thus excitable fibroblasts promise to be a useful alternative to cells that have been used previously in the study of cell-semiconductor coupling.

The authors are grateful to Dr. M. Denyer and Dr. M. Riehle for heart cell preparation protocols. The authors are grateful to Dr. R. Simson and D. Braun for helpful discussions and comments about the RICM and FLIC method and to S. Dannöhl for the AFM roughness measurements. We particularly thank Prof. G. ten Bruggencate for support and equipment.

This work was supported by BMBF Germany (grant 0310845A to WJP, MG, and HEG) and the Deutsche Forschungsgemeinschaft (JD, MR).

REFERENCES

Alberts, V. B., D. Bray, J. Lewis, M. Raff, K. Roberts, and J. D. Watson. 1994. Molecular Biology of the Cell. Garland, New York. .

Axelrod, D. 1981. Cell-substrate contacts illuminated by total internal reflection fluorescence. *J. Cell Biol.* 89:141–145.

Axelrod, D., T. P. Burghardt, and N. L. Thompson. 1984. Total internal reflection fluorescence. *Annu. Rev. Biophys. Bioeng.* 13:247–268.

Bereiter-Hahn, J., C. H. Fox, and B. Thoreli. 1979. Quantitative reflection contrast microscopy of living cells. *J. Cell. Biol.* 82:767–779.

Bergveld, P., J. Wiersma, and H. Meertens. 1976. Extracellular potential recordings by means of a field effect transistor without gate metal, called OSFET. *IEEE Trans. Biomed. Eng.* 23:136–144.

Blondel, B., I. Roijen, and J. P. Cheneval. 1971. Heart cells in culture: a simple method for increasing the proportion of myoblasts. *Experientia.* 27:356–358.

Bousse, L., D. Hafeman, and N. Tran. 1990. Time-dependence of the chemical response of silicon nitride surfaces. *Sensors Actuators B.* 1:361–367.

Bousse, L., and S. Mostarshed. 1991. The zeta potential of silicon nitride thin films. *J. Electroanal. Chem.* 302:269–274.

Braun, D., and P. Fromherz. 1997. Fluorescence interference-contrast microscopy of cell adhesion on oxidized silicon. *Appl. Phys. A.* 65: 341–348.

Butt, H. J., and M. Jaschke. 1995. Thermal noise in atomic force microscopy. *Nanotechnology.*

Cleveland, J. P., M. Radmacher, and P. K. Hansma. 1995. *In* Forces in Scanning Probe Methods. H. J. Güntherodt et al., editors. Kluwer Academic Publishers, Dordrecht, the Netherlands. 543–549.

Connolly, P., P. Clark, A. S. G. Curtis, J. A. T. Dow, and C. D. W. Wilkinson. 1990. An extracellular microelectrode array for monitoring electrogenic cells in culture. *Biosens. Bioelectron.* 5:223–234.

deRoos, A. D. G., P. H. G. M. Willems, P. H. J. Peters, E. J. J. V. Zoelen, and A. P. R. Theuvenet. 1997a. Synchronised calcium spiking resulting from spontaneous calcium action potentials in monolayers of NRK fibroblasts. *Cell Calcium.* 22:195–207.

deRoos, A. D. G., P. H. G. M. Willems, E. J. J. V. Zoelen, and A. P. R. Theuvenet. 1998. Synchronized Ca^{2+} signaling by intercellular propagation of Ca^{2+} action potentials in NRK fibroblasts. *Am. J. Physiol. C Cell Physiol.* 42:1900–1907.

deRoos, A. D. G., E. J. J. V. Zoelen, and A. P. R. Theuvenet. 1997b. Membrane depolarization in NRK fibroblasts by bradykinin is mediated by a calcium-dependent chloride conductance. *J. Cell. Physiol.* 170: 166–173.

Domke, J., and M. Radmacher. 1998. Measuring the elastic properties of thin polymer films with the atomic force microscope. *Langmuir.* 14: 3320–3325.

Donath, E., and D. Gingell. 1983. A sharp cell surface conformational transition at low ionic strength changes the nature of the adhesion of enzyme-treated red blood cells to a hydrocarbon interface. *J. Cell Sci.* 63:113–124.

Fromherz, P., A. Offenhäusser, T. Vetter, and J. Weis. 1991. A neuron-silicon junction: a Retzius cell of the leech on an insulated-gate filed-effect transistor. *Science.* 252:1290–1293.

Gingell, D., and I. Todd. 1979. Interference reflection microscopy—a quantitative theory for image interpretation and its application to cell-substratum separation measurement. *Biophys. J.* 26:507–526.

Gingell, D., and I. Todd. 1980. Red blood cell adhesion. II. Interferometric examination of the interaction with hydocarbon oil and glass. *J. Cell Sci.* 41:135–149.

Gingell, D., I. Todd, and J. Bailey. 1985. Topography of cell-glass apposition revealed by total internal reflection fluorescence of volume markers. *J. Cell Biol.* 100:1334–1338.

Gingell, D., and S. Vince. 1979. *In* The Third Symposium of the British Society for Cell Biology: Cell Adhesion and Motility. A. S. G. Curtis and J. D. Pitts, editors. Cambridge University Press, Cambridge. 1–37.

Gross, G. W., A. Harsch, B. K. Rhoades, and W. Göpel. 1997. Odor, drug and toxin analysis with neuronal networks in vitro: extracellular array recording of network responses. *Biosens. Bioelectron.* 12:373–393.

Gross, G. W., B. K. Rhoades, H. M. E. Azzazy, and M.-C. Wu. 1995. The use of neuronal networks on multielectrode arrays as biosensors. *Biosens. Bioelectron.* 10:553–567.

Gross, G. W., E. Rieske, G. W. Kreutzberg, and A. Meyer. 1977. A new fixed-array multi-microelectrode system designed for long-term monitoring of extracellular single unit neuronal activity in vitro. *Neurosci. Lett.* 6:101–105.

Gross, G. W., W. Y. Wen, and J. W. Lin. 1985. Transparent indium-tin oxide electrode patterns for extracellular, multisite recording in neuronal cultures. *J. Neurosci. Methods.* 15:243–252.

Hamill, O. P., A. Marty, E. Neher, B. Sakman, and F. J. Sigworth. 1981. Improved patch-clamp techniques for high-resolution current recording from cells and cell-free membrane patches. *Eur. J. Physiol. Pflügers Arch.* 391:85–100.

Harame, D. L., L. J. Bousse, J. D. Shott, and J. D. Meindl. 1987. Ion-sensing devices with silicon nitride and borosilicate glass insulators. *IEEE Trans. Electron Devices.* ED-34:1700–1707.

Hecht, E. 1987. Optics. Addison-Wesley, Reading, MA.

Henderson, E., P. G. Haydon, and D. S. Sakaguchi. 1992. Actin filament dynamics in living glial cell images by atomic force microskopy. *Science.* 257:1944–1946.

Hornung, J., and G. Fuhr. 1996. Influence of polylysine on adhesion of fibroblasts to glass substrates visualized by total internal reflection microscopy. *Exp. Biol. Online.* 1:.

Hornung, J., T. Müller, and G. Fuhr. 1996. Cryopreservation of anchorage-dependent mammalian cells fixed to structured glass and silicon substrates. *Cryobiology.* 33:260–270.

Israel, D. A., W. H. Barry, D. J. Edell, and R. G. Mark. 1984. An array of microelectrodes to stimulate and record from cardiac cells in culture. *Am. J. Physiol.* 247:H669–H674.

Israel, D. A., D. J. Edell, and R. G. Mark. 1990. Time delays in propagation of cardiac action potential. *Am. J. Physiol.* 258:H1906–H1917.

Izzard, C. S., and L. R. Lochner. 1976. Cell-to-substrate contacts in living fibroblasts: an interference reflection study with an evaluation of the technique. *J. Cell Sci.* 21:129–159.

Izzard, C. S., and L. R. Lochner. 1980. Formation of cell-to-substrate contacts during fibroblast motility: an interference-reflection study. *J. Cell Sci.* 42:81–116.

Jacobson, S. L., and H. M. Piper. 1986. Cell cultures of adult cardiomyocytes as models of the myocardium. *J. Mol. Cell. Cardiol.* 18:661–678.

Jimbo, Y., H. P. C. Robinson, and A. Kawana. 1993. Simultaneous measurements of intracellular calcium and electrical activity from patterned neural networks in culuture. *IEEE Trans. Biomed. Eng.* 40:804–810.

Johnson, S. J., T. M. Bayerl, D. C. McDermott, G. W. Adam, A. R. Rennie, R. K. Thomas, and E. Sackmann. 1991. Structure of an adsorbed dimyristoylphosphatidylcholine bilayer measured with specular deflection of neutrons. *Biophys. J.* 59:289.

Kodama, I., and M. Boyett. 1985. Regional differences in the electrical activity of the rabbit sinus node. *Pflügers Arch.* 404:214–226.

Lambacher, A., and P. Fromherz. 1996. Fluorescence interference-contrast microscopy on oxidized silicon using a monomolecular dye layer. *Appl. Phys. A Solids Surfaces.* 63:207–216.

Nathan, R. D. 1986. Two electrophysiologically distinct types of cultured pacemaker cells from rabbit sinoatrial node. *Am. J. Physiol.* 250: H325–H329.

Novak, J. L. 1986. Recording from the *Aplysia* abdominal ganglion with a planar microelectrode array. *IEEE Trans. Biomed. Eng.* 33:196–202.

Offenhäusser, A., C. Sprössler, M. Matsuzawa, and W. Knoll. 1997. Field-effect transistor array for monitoring electrical activity from mammalian neurons in culture. *Biosens. Bioelectron.* 12:819–826.

Pluta, M. 1988. Advanced Light Microscopy, Vol. 2, Specialized Methods. PWN-Polish Scientific Publishers, Warsaw.

Rädler, J., and E. Sackmann. 1992. On the measurement of weak repulsive and frictional colloidal forces by reflection interference contrast microscopy. *Langmuir.* 8:848–853.

Rädler, J., and E. Sackmann. 1993. Imaging optical thicknesses and separation distances of phospholipid vesicles at solid surfaces. *J. Physique II France.* 3:727–748.

Radmacher, M., R. W. Tillmann, M. Fritz, and H. E. Gaub. 1992. From molecules to cells: imaging soft samples with the atomic force microscope. *Science.* 257:1900–1905.

Regehr, W. G., J. Pine, C. S. Cohan, M. D. Mischke, and D. W. Tank. 1989. Sealing cultured invertebrate neurons to embedded dish electrodes facilitates long-term stimulation and recording. *J. Neurosci. Methods.* 30:91–106.

Riehle, M., and J. Bereiter-Hahn. 1994. Oubain and digitoxin as modulators of chick embryo cardiomyocytic energy metabolism. *Arzneimittel-Forschung/Drug Res.* 44:943–947.

Risso, S., and L. J. DeFelice. 1993. Ca channel kinetics during the spontaneous heart beat in embryonic chick ventricle cells. *Biophys. J.* 65: 1006–1018.

Schaffer, P., H. Ahammer, W. Müller, B. Koidl, and H. Windisch. 1994. Di-4-ANEPPS causes photodynamic damage to isolated cardiomyocytes. *Pflügers Arch.* 426:548–551.

Schindl, M., E. Wallraff, B. Deubzer, W. Witke, G. Gerisch, and E. Sackmann. 1995. Cell-substrate interactions and locomotion of *Dictyostelium* wild-type and mutants defective in three cytoskeletal proteins: a study using quantitative reflection interference contrast microscopy. *Biophys. J.* 68:1177–1190.

Simson, R., E. Wallraff, J. Faix, J. Niewöhner, G. Gerisch, and E. Sackmann. 1998. Membrane bending modulus and adhesion energy of wild-type and mutant cells of *Dictyostelium* lacking talin or cortexillins. *Biophys. J.* 74:514–522.

Thomas, C. A., P. A. Springer, G. E. Loeb, Y. Berwald-Netter, and L. M. Okun. 1972. A miniature microelectrode array to monitor the bioelectric activity of cultured cells. *Exp. Cell Res.* 74:61–66.

Vassanelli, S., and P. Fromherz. 1997. Neurons from rat brain coupled to transistors. *Appl. Phys. A.* 65:85–88.

Vassanelli, S., and P. Fromherz. 1998. Transistor records of excitable neurons from rat brain. *Appl. Phys. A.* 66:459–463.

Verschueren, H. 1985. Interference reflection microscopy in cell biology: methodology and applications. *J. Cell. Sci.* 75:279–301.

Wilson, R. J. A., L. Breckenridge, S. E. Blackshaw, P. Connolly, J. A. T. Dow, A. S. G. Curtis, and C. D. W. Wilkinson. 1994. Simultaneous multisite recordings and stimulation of single isolated leech neurons using planar extracellular electrode arrays. *J. Neurosci. Methods.* 53: 101–110.

Wolf, H., and D. Gingell. 1983. Conformational response of the glycocalyx to ionic strength and interaction with modified glass surface: a study of live red cells by interferometry. *J. Cell Sci.* 63:101–112.